Progress In Electromagnetics Research C, Vol. 61, 105–113, 2016

Wideband Dual-Polarized Omnidirectional Antenna with High Isolation for Indoor DAS Applications

Lei Zhou*, Yongchang Jiao, Zibin Weng, Yihong Qi, and Tao Ni

Abstract—A low-profile dual-polarized omnidirectional antenna is presented. The antenna is a combination of a vertically-polarized (VP) antenna and a horizontally-polarized (HP) antenna. The VP antenna is composed of a circular ground plane, a cross-shaped metal patch with four shorted legs and a top-loading circular ring. The printed dipoles of the HP antenna are fed through a three-way power divider etched on an FR4 substrate. To maintain stable radiation and reflection characteristics, the HP feed coaxial cable is soldered on one patch of the VP antenna to reduce the parasitic current on the feed cable. The VP antenna covers the frequency bands for GSM/2G/3G/4G LTE, and the HP antenna works in an overlapping frequency bands for 3G and 4G LTE communication systems with high isolation. The VP antenna achieves a wide bandwidth of 108% from 800 MHz to 2700 MHz, and its gains are larger than 2 dBi in 800∼960 MHz band and greater than 4 dBi in 1710∼2700 MHz band, respectively. The HP antenna works in the frequency band from 1700 MHz to 2700 MHz, and its gains are greater than 3 dBi. The proposed dual-polarized antenna is simulated, fabricated and measured. Measured results are in good agreement with the simulated ones.

1. INTRODUCTION

In recent years, with the rapid development of mobile communication systems, polarization diversity that uses a pair of antennas with orthogonal polarizations has been widely used in indoor distributed antenna system (DAS) [1]. In modern indoor DAS, there is an upsurge need for wide-band antennas to cover most widely used communication systems. The antennas should operate in 806∼960 MHz and 1710 ∼2690 MHz bands, which covers GSM, 3G, 4G LTE, WLAN and WiMAX bands [2].

Over the past years, various types of dual-polarized omnidirectional antennas have been introduced and discussed. In [3], a broadband vertically/horizontally dual-polarized omnidirectional antenna is proposed for mobile communication. The antenna is a combination of a modified low-profile monopole for vertically-polarized (VP) antenna and a circular planar loop for horizontally-polarized (HP) antenna. The VP and HP antennas are placed at both sides of ground plane. Once the antennas are mounted to the ceiling, a proper distance between the HP antenna and the ceiling is necessary for the antenna to work well, which will increase the total height in applications. A multiband dual-polarized omnidirectional antenna is proposed in [4]. The antenna is composed of a modified asymmetric biconical structure for the VP element, and a six-element printed dipole circular array for the HP element. However, its isolation is only about 25 dB. The antenna has relatively complex structures, and its HP element is etched on a large FR4 substrate, which will increase the manufacturing cost. Total height of the antenna is 117 mm ($0.227\lambda 0$, $\lambda 0$ is the free space wavelength at 800 MHz) and its radius is 100 mm ($0.267\lambda 0$). A novel broadband omnidirectional MIMO antenna is proposed in [5]. Its VP element consists of a discone antenna with a top-loading ring shorted to the ground plane and a round sleeve. The antenna

Received 1 December 2015, Accepted 29 December 2015, Scheduled 9 January 2016
* Corresponding author: Lei Zhou (lei.zhou.xd@hotmail.com).
The authors are with the National Key Laboratory of Antennas and Microwave Technology, Xidian University, Xi'an, Shaanxi 710071, P. R. China.

structure is complex, and high in cost. The isolation of the antenna is less than 25 dB. The HP feed coaxial routing type is not mentioned and its cross-polarization levels are not good enough at higher frequency band.

In this paper, we propose a wideband dual-polarized omnidirectional antenna with high isolation for modern indoor DAS applications. High isolation will result better throughput in the system. The VP antenna is a modified disk-monopole antenna with four shorted legs and a top-loading ring. In order to improve performance of the antenna radiation pattern ripples, also known as roundness, four arc-shaped shorted walls are added next to each shorted leg in the ground plane. The HP antenna is composed of three printed dipoles fed by a three-way power divider. The VP antenna is low in profile with a wide bandwidth of 108% from 800 to 2700 MHz. The HP antenna works in an overlapping frequency band ranging from 1700 to 2700 MHz. The antenna covers the GSM/2G/3G/4G LTE bands with high isolation and good cross-polarization levels. The proposed antenna is simulated, fabricated and measured.

2. ANTENNA DESIGN

2.1. Antenna Geometry

The 3D geometry of the proposed wideband dual-polarized omnidirectional antenna is illustrated in Figure 1(a). The related coordinate system and vectors $\mathbf{E}\theta$ and $\mathbf{E}\varphi$ are shown in Figure 1(a). As shown, the proposed antenna is simple in structure and easy to manufacture. The dual-polarized antenna is a combination of a VP antenna and a HP antenna. The distance between these two antennas is 40 mm, and the total height of the antenna is 85 mm ($0.227\lambda_0$), which is obviously lower than that of the antenna in [4]. The VP antenna mainly consists of two crossed patches with four shorted branches, a top-loading ring over the top of the patches, four arc-shaped walls located next to each shorted branches, and a circular ground plane. All patches are made of 1 mm-thick aluminum or copper. The radius of the ground plane is 125 mm ($0.333\lambda_0$), and the height of the VP antenna is about 45 mm. Detailed dimensions of the VP antenna are shown in Figure 1(b). The feed point of the VP antenna is located at the center of the ground plane. Once the VP antenna is excited, a disk-monopole like radiation patterns will be obtained. Four shorted legs and the top-loading ring are designed to reduce the profile and enhance the bandwidth of the VP antenna. By adding four arc-shaped walls along each shorted leg, good radiation characteristics of the VP antenna are achieved.

Figures 1(c) and 1(d) show the prototype of the HP antenna. The HP antenna is composed of

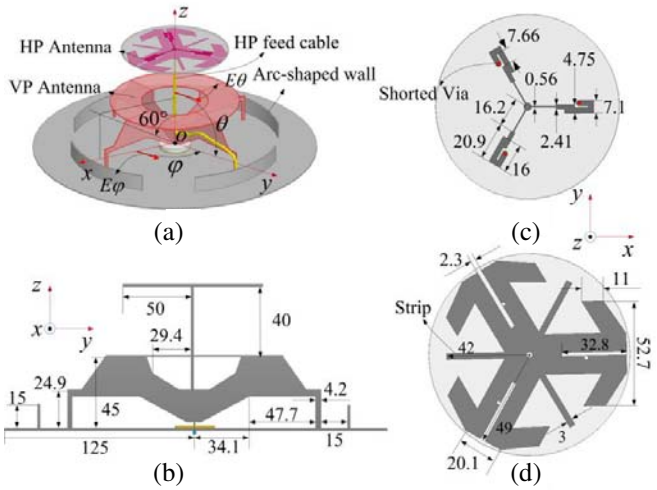

Figure 1. Geometry of the proposed antenna. (a) Overview of the proposed antenna, (b) Cross-section view of the proposed antenna, (c) Top view of the HP antenna, and (d) Bottom view of the HP antenna (Unit: mm).

three printed dipoles, which are excited by a simplified broadband three-way power divider with three shorted via holes. Both parts are etched on an FR4 substrate (Thickness=2 mm, $\varepsilon_r = 4.4$, loss tangent = 0.02). These three dipoles are printed on the bottom side of the substrate, and the feeding network is etched on its top side. Three strips are added between each pairs of dipoles to improve the radiation performance.

2.2. VP Antenna Design

The geometry of the proposed VP antenna is shown in Figure 2(c). The antenna is composed of a ground plane, crossed patches, a top-loading ring and four arc-shaped walls. Figure 2(a) shows the fabrication of the crossed patches, and both patches are made of 1 mm-thick copper and connected together by using soldering process. The top-loading ring is fixed on the crossed patches and the arc-shaped walls are put next to each shorted branches.

Figure 2 also shows the evolution process for designing the wideband low-cost omnidirectional VP antenna. Figure 2(a) shows a disk-like monopole antenna, which is composed of two crossed patches and a circular ground plane. This antenna operates only in the higher frequency band. Then, four shorted legs are added at the end of each patch, as shown in Figure 2(b). This method effectively extends the lower frequency band. In order to further reduce the lowest resonant frequency, a top-loading ring is added on the top of two patches. Figure 3(a) gives a comparison of the reflection coefficients between the proposed VP antenna and two original antennas. It can be seen that the lowest resonant frequency decreases by adding shorted branches and top-loading ring. Figure 3(b) presents the current distributions on three different VP antennas. As shown in the figure, the current densities on the area near the shorted legs become strong at 800 MHz for Ant 2 and Ant 3. Figure 4 shows the electric current sheet **J** of Ant 1 and Ant 3. Figure 4(a) indicates that Ant 1 radiates in a manner similar to a conventional vertically polarized disk-monopole antenna and demonstrates an omnidirectional pattern at 1700 MHz. Once the shorted branches are added, a loop will be formed. The current which flows along the loop demonstrates a virtual magnetic current sheets **M** at 800 MHz. According to Huygen's principle, the current sheet **M** has the same polarization with current sheet **J**. The current distribution of Ant 1 also demonstrates that the proposed antenna only works in the high frequency band without

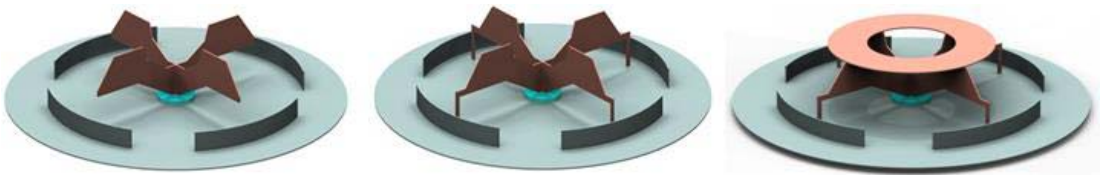

(a) Ant 1 (b) Ant 2 (c) Ant 3

Figure 2. Three different VP antennas.

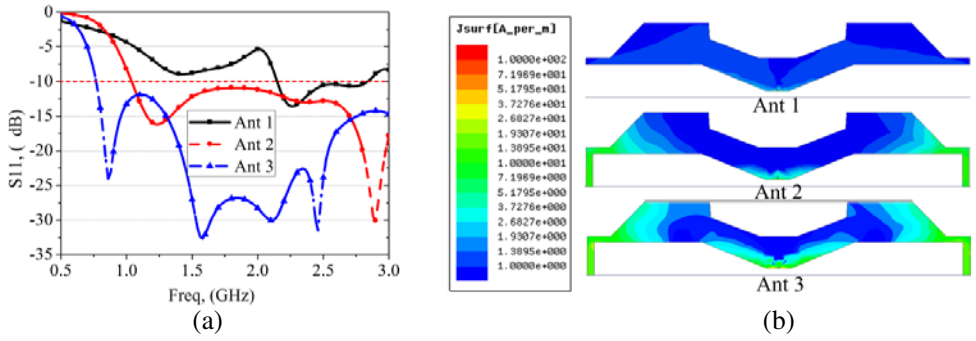

(a) (b)

Figure 3. Reflection coefficients and current distributions of three different VP antennas. (a) Reflection coefficients and (b) Current distributions (800 MHz).

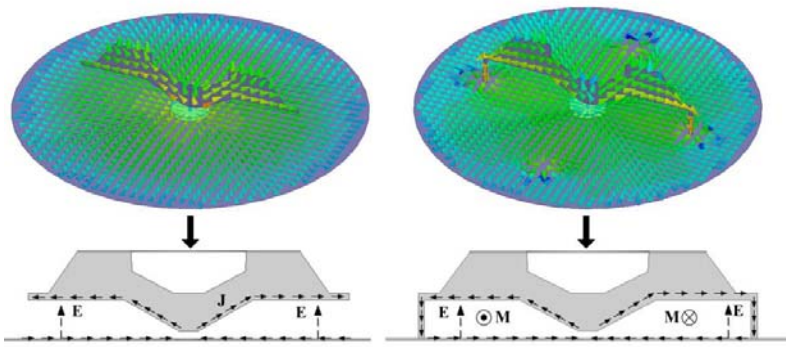

(a) Ant 1 (b) Ant 3

Figure 4. Surface **J** fields of Ant 1 and Ant 3. (a) Electric current sheet **J** of Ant 1 (1700 MHz) and (b) Magnetic current sheet **M** of Ant 3 (800 MHz).

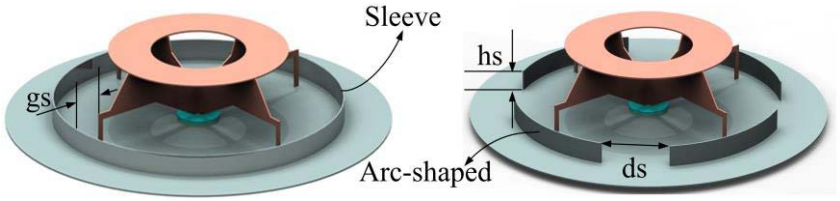

(a) Circular sleeve reflector (b) Arc-shaped metal wall

Figure 5. Proposed antenna with different kinds of reflectors.

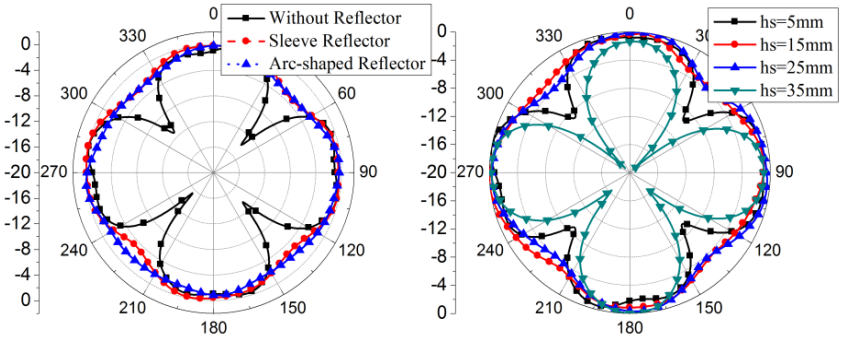

(a) (b)

Figure 6. Horizontal radiation patterns of the VP antenna at 2700 MHz. (a) Comparison of the horizontal radiation patterns between the proposed VP antenna and two original antennas, and (b) Effect of parameter h_s on horizontal radiation patterns of the antenna.

shorted branches. Once the branches are added, the antenna achieves a magnetic mode in the lower frequency band. Above all, profile of the VP antenna is reduced efficiently by adding four shorted legs and one top-loading ring.

In order to make the antenna radiate uniformly in the horizontal plane, a sleeve structure is used, as shown in Figure 5(a). The circular sleeve structure is simplified by four arc-shaped metal walls, as shown in Figure 5(b). Figure 6(a) indicates that the horizontal radiation patterns have little difference between the circular sleeve and arc-shaped metal walls. If the walls are removed, the horizontal radiation pattern ripples will get worse. The ripples of the antenna will increase from 3.5 dB to 15 dB at 2700 MHz. For cost and manufacturing considerations, the sleeve reflector is replaced by four arc-shaped metal walls. Figure 6(b) demonstrates that the horizontal radiation pattern ripple can be optimized by varying hs

values. With the increase of hs value, the horizontal radiation ripples initially get reduced and then increased. If ds is less than 120 mm, it will have little influence on radiation patterns. By optimizing the position and dimensions of the walls, good H-plane radiation patterns are obtained with little influence on VSWRs.

2.3. HP Antenna Design

In the HP antenna design, three printed dipoles are fed through a three-way power divider etched on an FR4 substrate, as shown in Figures 1(c) and 1(d). The HP antenna covers a wide band from 1700 to 2700 MHz. The feeding network is composed of three broadband baluns with three short-circuits and an impedance matching circuit. The HP antenna has the lightning protection feature for practical applications. This type of broadband balun consists of a slot line etched on the bottom side of the substrate and a -shaped microstrip line etched on its top side, which has been widely used in printed dipoles. The slot-microstrip coupling structure enhances the impedance bandwidth of the printed dipoles. Three parasitic strips are added to improve the cross-polarization performance at higher frequency band.

There are always common mode currents on the HP feed coaxial cable, which are caused by the imbalance of the antenna or measurement setups. The common mode current on the testing cable always contributes a few undesired parasitic radiations of omnidirectional antennas and affects the reflection performance either. To keep stable radiation and reflection characteristics, the HP feed coaxial cable is soldered on one patch of the VP antenna along the red dashed line, as shown in Figure 7(a). This method keeps the structure symmetric in the antenna design, and the parasitic common currents of the HP feed cable are reduced efficiently. Another bending type of the HP coaxial cable, indicated by the blue solid line, is shown in Figure 7(a). The bending Type B has obvious influence on the horizontal radiation patterns of the VP antenna, as shown in Figure 8. Type B worsens ripples of the VP antenna obviously.

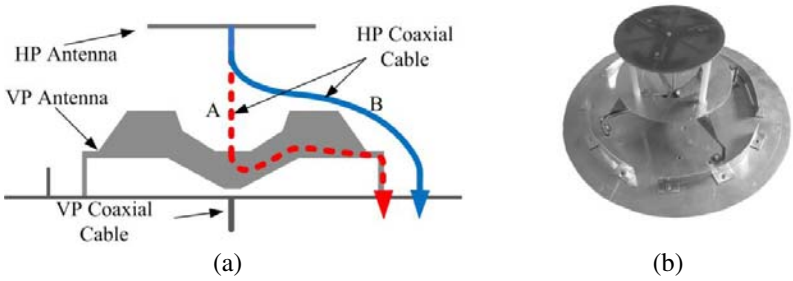

Figure 7. Manufacture of the proposed antenna. (a) Fabrication of the feed coaxial cable for the HP antenna, (b) Photograph of the proposed antenna.

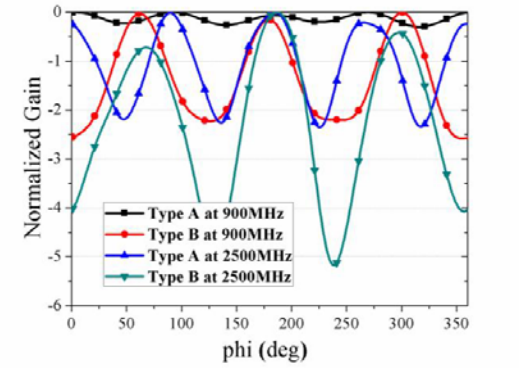

Figure 8. Effect of bending types of feed coaxial cable for the HP antenna on the horizontal radiation patterns of the VP antenna.

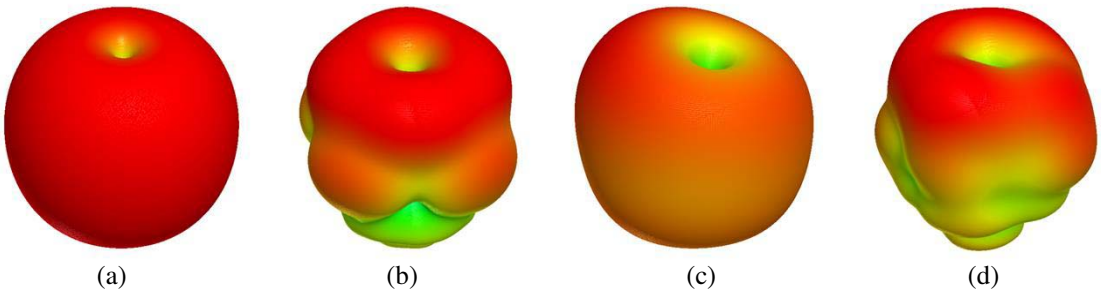

Figure 9. Radiation patterns for the VP antennas. (a) Type A at 900 MHz, (b) Type A at 2500 MHz, (c) Type B at 900 MHz, and (d) Type B at 2500 MHz.

Figure 9 shows 3D VP radiation patterns at 900 MHz and 2500 MHz for Types A and B respectively. Figures 9(a) and 9(b) indicate that the radiation patterns for Type A are uniform in the horizontal plane at both 900 and 2500 MHz frequency points. It can be seen that the maximum gain direction tilts to the z-axis at higher frequency band. Once the HP feed coaxial cable is routed as Type B, the omnidirectional performance will get worse, as shown in Figures 9(c) and 9(d), thus the gains increase from 1.66 dBi to 3 dBi at 900 MHz, and 7.3 dBi to 8.25 dBi at 2500 MHz, respectively. Considering the uniformity of the radiation patterns, we conclude that Type A is better than Type B.

3. SIMULATED AND MEASURED RESULTS

The proposed dual-polarized antenna is simulated, fabricated and measured. S-parameters and radiation patterns of the proposed antenna is simulated by using ANSYS HFSS 15. S-parameters are measured by using Agilent E5071C Network Analyser, and the radiation patterns are measured by a far-field antenna measurement system.

3.1. Reflection Coefficients

The simulated and measured S-parameter results are shown in Figure 10. It can be seen that both the simulated and measured reflection coefficients for the VP antenna are better than -10 dB over the whole frequency band from 800 to 2700 MHz. The achieved impedance bandwidth for $|S_{\mathrm{hh}}| < -10$ dB for the HP antenna is 45.5% from 1700 to 2700 MHz. The isolation between VP and HP ports is better than 38 dB over the whole frequency band.

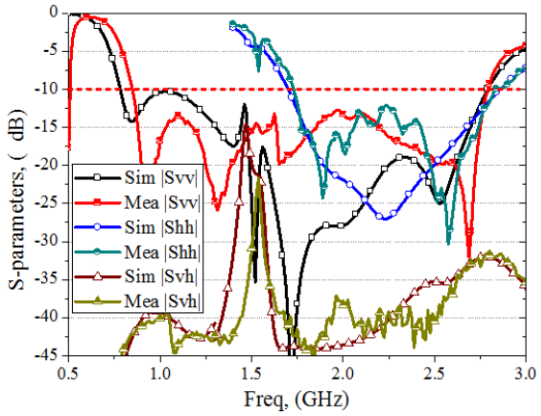

Figure 10. Simulated and measured S-parameters of the proposed antenna.

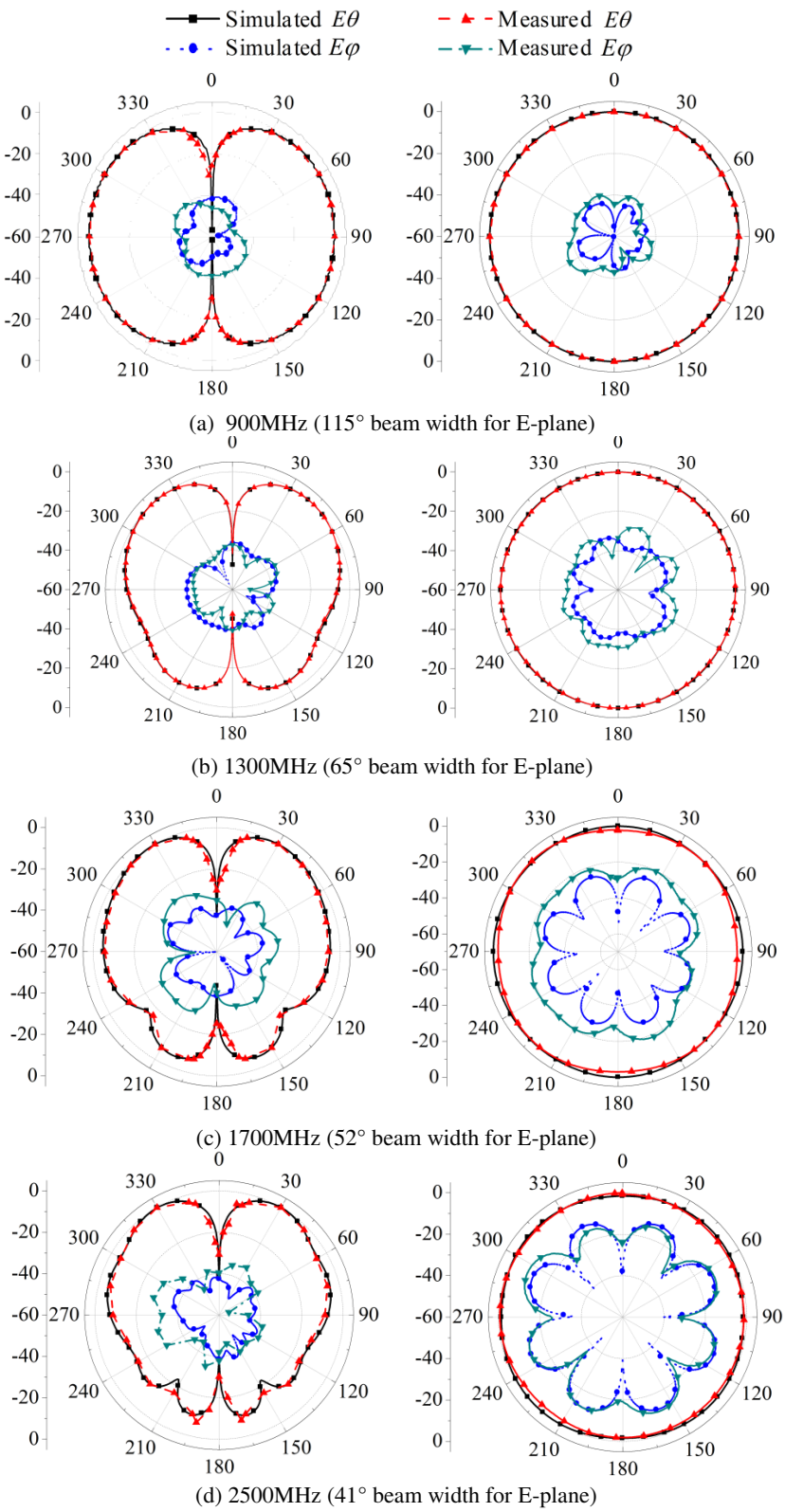

Figure 11. Simulated and measured radiation patterns for the VP antenna. (a) 900 MHz, (b) 1300 MHz, (c) 1700 MHz and (d) 2500 MHz.

3.2. Radiation Patterns

Simulated and measured radiation patterns for VP and HP antennas are shown in Figures 11 and 12. Both VP and HP antennas show omnidirectional characteristics in the horizontal plane. The measured E-plane radiation patterns for the VP antenna are shown in the left side of Figure 11. The measured 3 dB beam width of the E-plane are 80∼115° for 800∼960 MHz band, and 40∼60° for 1700∼2700 MHz band, respectively. The measured H-plane radiation patterns for the VP antenna are shown in the right side of Figure 11. The horizontal pattern ripples of the proposed antenna are less than 0.5 dB for 800∼960 MHz band, and 3.5 dB for 1700∼2700 MHz band, respectively.

Figure 12 shows the simulated and measured radiation patterns for the HP antenna at 1700 MHz and 2500 MHz. The H-plane radiation patterns have good roundness performance for ripples less than 4 dB. Over the whole overlapping frequency band, the co-polarization levels are 11 dB greater than the cross-polarization levels for the VP antenna and 10 dB for the HP antenna in the horizontal plane.

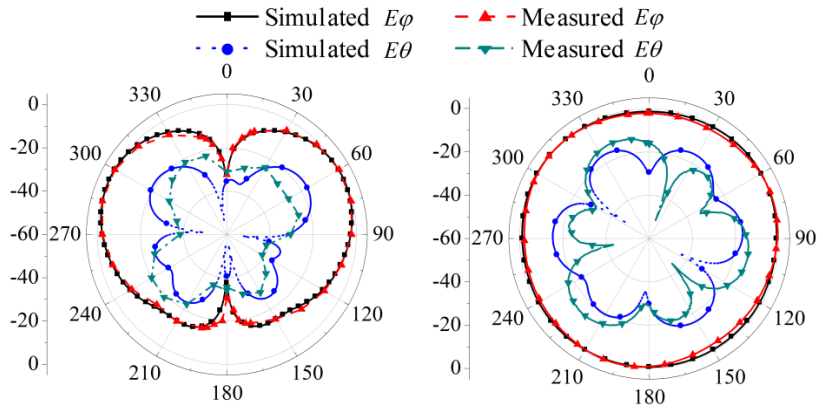

(a) 1700MHz (57° beam width for H-plane)

(b) 2500MHz (69° beam width for H-plane)

Figure 12. Simulated and measured radiation patterns for the HP antenna. (a) 1700 MHz, and (b) 2500 MHz.

Figure 13 shows the simulated and measured gain results. Good agreement between simulation and measurement is observed. The achieved gains of the VP antenna are larger than 1.5 dBi in lower frequency band, and 4.2 dBi in higher frequency band, respectively. In the overlapping frequency band, the gains of the HP antenna vary from 3 to 5 dBi. From 1700 to 2700 MHz, both VP and HP antenna gains increase first and then decrease. Figure 13 also shows measured efficiencies of the proposed antenna. It can be seen that the efficiencies are larger than 80% and 75% for VP and HP antennas, respectively. Both VP and HP antenna efficiencies decrease at higher frequency band. Due to the length of the HP feed coaxial is longer than that of the VP antenna, the VP antenna efficiency is larger than the HP antenna efficiency over the whole overlapping frequency band. The dual polarized radiation patterns and gains are helpful for the capacity and coverage of the indoor MIMO system.

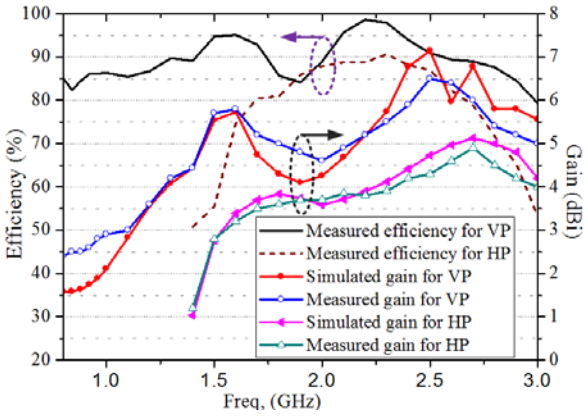

Figure 13. Gains and realized radiation efficiencies of the proposed antenna.

4. CONCLUSION

An innovative wideband dual-polarized omnidirectional antenna with high isolation and good cross polarization levels has been introduced. The VP antenna is a modified disk-monopole antenna with four shorted legs. Four arc-shaped shorted walls are added to improve the radiation performance of the VP antenna. The HP antenna is composed of three printed dipoles, which are fed by a wideband three-way power divider. To keep stable radiation and reflection characteristics, the HP feed coaxial cable is soldered on one patch of the VP antenna. The VP antenna is low in profile with a wide bandwidth of 108% (800∼2700 MHz), and the HP antenna works in the overlapping frequency band from 1700 MHz to 2700 MHz. The isolation between VP and HP ports is larger than 38 dB. The operating bands cover the GSM900, GSM1800, UMTS2100 and LTE bands. The proposed antenna is simulated, fabricated and measured. The antenna has a high isolation between two ports and stable radiation patterns with good cross-polarization levels over the whole frequency band. The low profile design makes it a good candidate for installing in public places. The proposed antenna can be widely used in indoor distributed systems for its excellent performance.

REFERENCES

1. Ando, A., A. kondo, and S. J. Kubota, "A study of ratio zone length of dual-polarized omnidirectional antennas mounted on rooftop for personal handy-phone system," *IEEE Trans. Antennas and Propag.*, Vol. 57, No. 1, 2–10, Jan. 2008.
2. "Technical specifications and group radio access network; user equipment (UE) radio transmission and reception (FD/TDD)," *Release 9, Third Generation Partnership Project (3GPP)*, TS. 25. 101/102/104/105. V9.5.0, 2010.
3. Quan, X. L. and R. L. Li, "A broadband dual-polarized omnidirectional antenna for base stations," *IEEE Trans. Antennas and Propag.*, Vol. 61, No. 2, 943–947, Feb. 2013.
4. Dai, X. W., Z. Y. Wang, C. H. Liang, X. Chen, and L. T. Wang, "Multiband and dual-polarized omnidirectional antenna for 2G/3G/LTE application," *IEEE Antennas Wireless Propag. Lett.*, Vol. 12, 1492–1495, 2013.
5. Jolani, F., Y. Q. Yu, and Z. Z. Chen, "A novel broadband omnidirectional dual polarized MIMO antenna for 4G LTE applications," *2014 IEEE International Wireless Symposium (IWS)*, 1–4, 2014.